



ELSEVIER

Available online at www.sciencedirect.com

SCIENCE @ DIRECT®

PALAEO

Palaeogeography, Palaeoclimatology, Palaeoecology xx (2005) xxx–xxx

www.elsevier.com/locate/palaeo

1

2 Resolving a late Oligocene conundrum: Deep-sea warming and 3 Antarctic glaciation

4 Stephen F. Pekar^{a,b,*}, Robert M. DeConto^c, David M. Harwood^d

5 ^a Queens College, School of Earth and Environmental Sciences, CUNY, 65-30 Kissena Blvd., Flushing, New York 11367, USA

6 ^b Lamont-Doherty Earth Observatory of Columbia University, Palisades, New York 10964, USA

7 ^c Department of Geosciences, 233 Morrill Science Center, University of Massachusetts, 611 North Pleasant Street, Amherst, MA 01003, USA

8 ^d Department of Geosciences, 214 Bessey Hall, University of Nebraska-Lincoln, Lincoln, NE 68588, USA

9 Received 2 December 2004; accepted 8 July 2005

10

11 Abstract

12 Changes in ice volume and the resulting changes in sea level were determined for the late Oligocene (26–23 Ma, Astronomical
13 Timescale, ATS) by applying $\delta^{18}\text{O}$ -to-sea-level calibrations to deep-sea $\delta^{18}\text{O}$ records from ODP Sites 689, 690, 929, 1090, and
14 1218. Our results show that maximum global ice volume occurred during two late Oligocene $\delta^{18}\text{O}$ events, Oi2c (24.4 Ma) and Mi1
15 (23.0 Ma) (inferred glacioeustatic lowering), with volumes up to ~25% greater than the present-day East Antarctic Ice Sheet
16 (EAIS). Ice volume during glacial minima was on the order of about 50% of the present-day EAIS. This is supported by late
17 Oligocene stratigraphic records from Antarctica that contain evidence of cold climates and repeated episodes of glaciation at sea
18 level and grounding lines of glacial ice on the Antarctic continental shelf in the Ross Sea and Prydz Bay. In contrast, composite
19 deep-sea $\delta^{18}\text{O}$ records show a significant decrease ($\geq 1\text{‰}$) between 26.7 and 23.5 Ma, which have long been interpreted as
20 bottom-water warming combined with deglaciation of Antarctica. However, a close examination of individual $\delta^{18}\text{O}$ records
21 indicates a clear divergence after 26.8 Ma between records from Southern Ocean locations (i.e., Ocean Drilling Program Sites 689,
22 690, 744) and those of other ocean basins. High $\delta^{18}\text{O}$ values (2.9‰–3.3‰) from these Southern Ocean $\delta^{18}\text{O}$ records are consistent
23 with an ice sheet on the East Antarctic continent equivalent to present-day values and cold bottom-water temperatures ($\leq 2.0\text{ °C}$).
24 These differences suggest a reduction in deep-water produced near the Antarctic continent (i.e., proto-Antarctic Bottom Water,
25 proto-AABW), which were quickly entrained and mixed with warmer (and presumably more saline) bottom-water originating from
26 lower latitudes. Expansion of a warmer deep-water mass and the weakening of the proto-AABW may explain the large intra-
27 basinal isotopic gradients that developed among late Oligocene benthic $\delta^{18}\text{O}$ records. These conclusions are also supported by
28 ocean modeling suggesting a reduction of deep-water formed in the Southern Ocean, strengthening of deep-water from the northern
29 hemisphere, and decreasing temperatures in high southern latitudes occurred as the Drake Passage opened to deep-water. Low $\delta^{18}\text{O}$
30 values reported from deep-sea locations other than the Southern Ocean are shown to bias estimates of Antarctic ice volume, calling
31 for a re-evaluation of the notion that Antarctic ice volume was significantly reduced during the late Oligocene.

32 © 2005 Published by Elsevier B.V.

33 **Keywords:** Oligocene; Oxygen isotopes; Sea-level; Ice volume; Antarctica

34

* Corresponding author. Queens College, School of Earth and Environmental Sciences, CUNY, 65-30 Kissena Blvd., Flushing, New York 11367, U.S.A. Tel.: +1 718 997 3305; fax: +1 718 997 3329.

E-mail address: spekar@qc1.qc.edu (S.F. Pekar).

35 1. Introduction

36 For decades, palaeoceanographers observed a significant
37 decrease in $\delta^{18}\text{O}$ values in late Oligocene com-

38 posite deep-sea records (e.g., Miller et al., 1987; Zachos
39 et al., 2001), which was generally attributed to deep-sea
40 warming, combined with a significant decrease in Ant-
41 arctic ice volume (e.g., Zachos et al., 2001). This
42 interpretation is supported by the assumption that bot-
43 tom-water emanated mainly from a Southern Ocean
44 source (i.e., Southern Component Water, presumably
45 originating around the Antarctic margin) during the
46 Oligocene (e.g., Wright and Miller, 1993); thus, serving
47 as a proxy for palaeoenvironmental conditions on the
48 Antarctic continent. Isotopic records from recently
49 cored ODP sites (Sites 1090 and 1218) contain higher
50 values, but are still near the threshold for requiring the
51 presence of an ice sheet (2.45‰; Miller et al., 1987).

52 In contrast, results from recent stratigraphic drilling
53 of the Antarctic continental margin (e.g., CIROS-1,
54 Cape Roberts Project) indicate a gradual and steady
55 Antarctic cooling during the Oligocene, culminating
56 in near tundra-like conditions by early Miocene (e.g.,
57 Raine, 1998; Raine and Askin, 2001; Thorn, 2001; Roberts
58 et al., 2003; Prebble et al., this issue). Palaeoenviron-
59 mental evidence from these terrestrial palynological and
60 phytolith data, as well as the sedimentary record from
61 glacial sediments recovered in upper Oligocene
62 strata from the western Ross Sea indicates that Antarc-
63 tica was sufficiently cold to support the existence of ice
64 sheets at sea level (e.g., Barrett, 1989; Cape Roberts
65 Science Team, 1998, 1999, 2000; Naish et al., 2001).
66 Identification of ice grounding lines near the shelf edge
67 near Prydz Bay as early as the early Oligocene (Cooper
68 et al., 1991; Bartek et al., 1997) also suggests the
69 presence of large continental ice sheets on East Antarc-
70 tica at this time. Additionally, eustatic estimates from
71 sequence stratigraphic records (Kominz and Pekar,
72 2001) indicate repeated sea-level lowerings during the

late Oligocene (25.1–23.0 Ma) consistent with a heavi- 73
ly glaciated East Antarctic continent (EAC) (Pekar et al., 74
2002). 75

This paper addresses the paradox of low $\delta^{18}\text{O}$ values 76
in deep-sea records coeval with proximal Antarctic 77
records suggesting decreasing and persistent cold tem- 78
peratures and large-scale ice sheets on East Antarctica. 79
Here we show that while ice volume may have fluctu- 80
ated on orbital timescales, Antarctica could have 81
remained mostly glaciated (equivalent to ~50% to 82
125% of present-day EAIS) throughout the late Oligo- 83
cene. We also suggest that the apparent late Oligocene 84
warming interpreted from deep-sea $\delta^{18}\text{O}$ records could 85
have been caused by an expansion of warmer deep- 86
water into most of the world's ocean basins, with colder 87
deep-water becoming entrained with and mixed into 88
this warmer deep-water mass. 89

2. Methods, definitions, and sites used in this study 90

Oxygen isotope records from DSDP and ODP Sites 91
522 (Miller et al., 1988), 529 (Miller et al., 1991), 558 92
(Miller and Fairbanks, 1983), 563 (Miller and Thomas, 93
1985), 689 (Kennett and Stott, 1990), 690 (Kennett and 94
Stott, 1990), 744 (Zachos et al., 2001), 747 (Wright et 95
al., 1992), 748 (Zachos et al., 1992), 754 (Zachos et al., 96
2001), 803 (Barrera et al., 1993), 929 (Zachos et al., 97
2001), 1090 (Billups et al., 2002), and 1218 (Lear et al., 98
2004) were used in this study (Fig. 1). Chronologies for 99
these records were previously developed by integrating 100
biostratigraphy and magnetostratigraphy, which have 101
been converted to the new Astronomical Time Scale 102
(ATS) of Laskar et al. (2005). These original age mod- 103
els vary in their uncertainties, which can affect the 104
development of time slice isotopic transects. However, 105

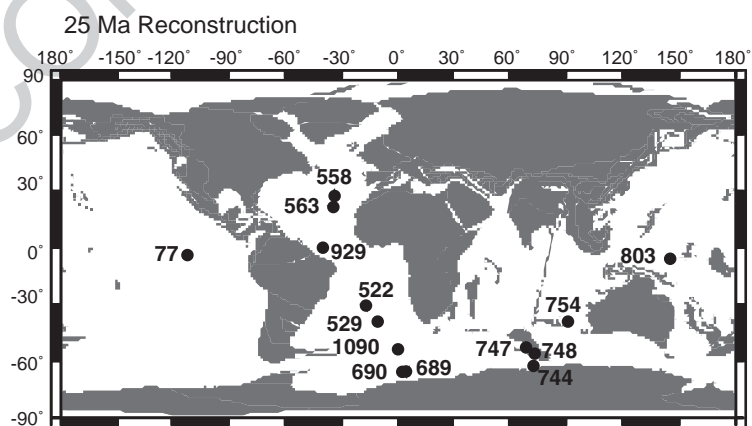


Fig. 1. Map showing plate tectonic reconstructions at circa 25 Ma (from Hay et al., 1999) with the palaeo-locations of DSDP and ODP sites used in this study.

106 each time slice includes a 400 ky interval across each
107 $\delta^{18}\text{O}$ event, which should be a sufficient length of time
108 to capture isotopic values representative of the event.

109 For Sites 689 and 690, which contain two important
110 isotopic records for the interpretations in this study,
111 Florindo and Roberts (2005) provided new chronostratigraphic
112 interpretations using u-channel samples for the upper Oligocene.
113 Although their new age models do not significantly alter late Oligocene
114 ages for Site 689, ages near the top of the Oligocene section in Site
115 690 are approximately 0.3 m.y. younger than previous
116 age models (e.g., Zachos et al., 2001). In Florindo and
117 Roberts (2005), the top of Chron 8n (25.1 Ma, ATS)
118 has been assigned to a change from normal to reversed
119 polarity at 55.0 mbsf. Therefore, an interval of normal
120 polarity occurring between 54.8 and 53.2 mbsf (Speiss,
121 1990) is assigned to Chron 7a (25.0–24.8 Ma) and a
122 short interval of normal polarity that begins immediately
123 below an unconformity at ~50 mbsf is assigned to
124 Chron 7n (24.5–24.1 Ma). The last isotope measurement
125 at Site 690 is obtained from a sample taken at
126 50.75 mbsf, which occurs within the lower portion of
127 Chron 7n and is therefore assigned an age of ~24.5 Ma.

128 Deep-sea isotopic values are typically obtained for
129 a single species, such as *Cibicidoides* spp. However,
130 *Cibicidoides* spp. as do most other benthic foraminifers
131 precipitate their tests out of equilibrium with calcite
132 ($\delta^{18}\text{O}$ values in the tests of *Cibicidoides* spp. are
133 offset with respect to calcite by + 0.64‰). All $\delta^{18}\text{O}$
134 records have been adjusted to represent the isotopic
135 value of calcite for samples reported either by previous
136 authors (i.e., Zachos et al., 2001) or in this study
137 (i.e., Site 1090).

138 The term apparent sea level (ASL) is used here and
139 is defined as eustasy plus the water-loading effects on
140 the crust (eustasy*~1.48; Pekar et al., 2002). The
141 maximum size of a fully glaciated East Antarctic continent
142 during the Oligocene is estimated to be equivalent to ≤ 80 m
143 ASL. This is based on $\delta^{18}\text{O}$ to ASL calibrations (Pekar et al.,
144 2002), coupled $\delta^{18}\text{O}$ and Mg/Ca ratio records by Lear et al.
145 (2000), and two-dimensional flexural backstripping and
146 stratigraphic studies (Kominz and Pekar, 2001). This ice
147 volume estimate is somewhat greater than recent GCM-ice
148 sheet simulations of the Oi1 event (DeConto and Pollard,
149 2003a), which ignored significant ice on West Antarctica
150 and the seaward expansion of grounding lines beyond the
151 model shorelines, and is closer to simulations of maximum
152 Antarctic ice volume during Quaternary glacial periods
153 (Ritz et al., 2001), when the total area of grounded ice
154 on East and West Antarctica was 15%–25% greater than
155 today (Denton and Hughes, 2002;

158 Huybrechts, 2002). Calibrations of $\delta^{18}\text{O}$ to ASL amplitudes
159 use detrended ASL estimates from Pekar et al. (2002) and
160 benthic foraminiferal $\delta^{18}\text{O}$ amplitudes at Oi- and Mi-events
161 (Miller et al., 1991; Pekar and Miller, 1996) from ODP
162 Sites 689, 690, 744, 929, and 1218 (Fig. 2; Pekar et al.,
163 2002). Detrended ASL estimates were derived by integrating
164 two-dimensional flexural backstripping (Kominz and Pekar,
165 2001) with two-dimensional palaeoslope modeling of
166 foraminiferal biofacies and lithofacies (Pekar and Kominz,
167 2001). Lowest calibrations are from the Weddell Sea ODP
168 Sites 690 and 689 (0.12‰/10 m ASL, $r^2=0.92$ and
169 0.13‰/10 m ASL, $r^2=0.72$, respectively), with higher
170 values for Sites 1218 (0.16‰/10 m ASL, $r^2=.67$) and
171 744 (0.26‰/10 m ASL, $r^2=0.82$) (Fig. 2). The calibrations
172 for Sites 929 and 1090 use a single $\delta^{18}\text{O}$ event (Mi1,
173 23.0 Ma). This results in a calibration ranging from
174 ~-0.2‰ to 0.5‰ (0.35‰ \pm 0.15‰ mean calibration) and
175 0.18‰ to 0.46‰ (0.32‰ \pm 0.14‰ mean calibration) per
176 10 m ASL for Sites 929 and 1090, respectively, based on
177 an ASL estimate of 56 ± 25 m. Differences among these
178 calibrations are attributable to greater variability in deep-sea
179 temperatures between glacial maxima and minima at the
180 million-year time-scale. The temperature signal within the
181 observed isotopic shifts ranges from 25% at Site 690 to
182 ~75% at Site 929, which is estimated by subtracting the
183 ice volume contribution (estimated to be 0.091‰/10 m
184 ASL, DeConto and Pollard, 2003a) from $\delta^{18}\text{O}$ to sea-level
185 calibrations.

186 For estimating Oligocene ice volume, $\delta^{18}\text{O}$ values of
187 3.0‰ or greater in deep-sea records are consistent with
188 a fully glaciated EAIS and cold bottom-water temperatures
189 (~-2.0 °C). This is based on the following. The modern
190 *Cibicidoides* spp. value in ~-2.0 °C water is 2.7‰
191 (Shackleton and Kennett, 1975) or 3.34‰ adjusted for
192 equilibrium. Of that value, the isotopic contribution from
193 the present-day ice sheets is estimated to range from
194 ~-0.9‰ to 1.2‰ (e.g., Miller et al., 1991; Zachos et al.,
195 2001). In this study, the isotopic contribution of the
196 present-day ice sheets is estimated to be ~-1.0‰, based
197 on present-day ice volume estimates from Williams and
198 Ferrigno (1999) (Table 1), using both grounded ice and
199 ice below sea level. Of that 1.0‰ value, 0.13‰ is
200 attributed to ice from Greenland and West Antarctica
201 (Table 1). This value includes average isotopic values of
202 the present-day West Antarctic and Greenland ice sheets
203 of approximately -30‰ and -39‰, respectively (obtained
204 by taking the average values of $\delta^{18}\text{O}$ records from ice
205 cores for each area). During the late Oligocene, Greenland
206 and West Antarctica may not have been glaciated, reducing
207 208 209

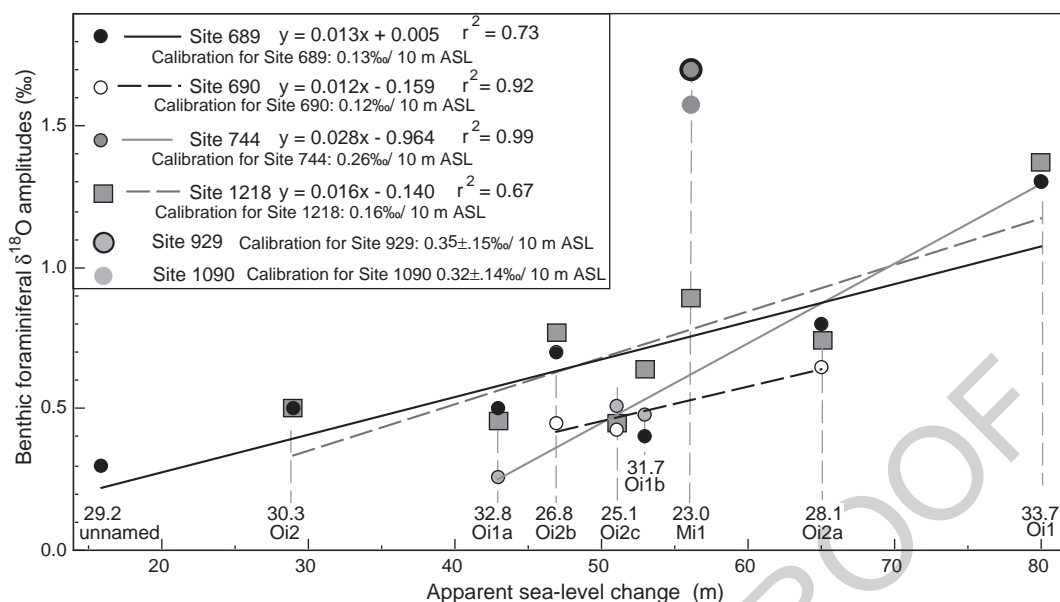


Fig. 2. Oxygen isotope amplitudes from Oi-events identified in ODP Sites 690, 689, 744, 929, 1090, and 1218 (Thomas et al., 1995; Zachos et al., 2001; Lear et al., 2004) are compared to detrended ASL amplitudes (Pekar et al., 2002). Oxygen isotope amplitudes are the difference between the maximum value of $\delta^{18}\text{O}$ event and preceding minimum (or average minimum) $\delta^{18}\text{O}$ value. ASL amplitudes (Pekar et al., 2002) are the difference between sea-level minimum and the preceding sea-level maximum. Oxygen isotope events and their ages are shown (Miller et al., 1991; Pekar and Miller, 1996). These correlations suggest that although benthic foraminiferal records are assumed to contain a significant bottom-water temperature signal, lowering of temperature results in a nearly linear increase in ice volume estimates. The $\delta^{18}\text{O}$ amplitude from Sites 929 and 1090 is calibrated to ASL with a single $\delta^{18}\text{O}$ event, which results in a larger uncertainty. It is also uncertain whether these calibrations would remain constant between high frequency (e.g., obliquity timescales) and million-year timescale (e.g., Oi- and Mi-events of Miller et al., 1991).

210 this average deep-sea $\delta^{18}\text{O}$ value by 0.13‰. Further-
 211 more, a wet-based, polythermal East Antarctic ice
 212 sheet, such as thought to have existed during the Oli-
 213 gocene, likely had significantly higher $\delta^{18}\text{O}$ values in
 214 the ice sheet (e.g., $\sim 35\text{‰}$) than values today (i.e., $-$
 215 45‰ to -55‰). We estimate that this would have
 216 further reduced the isotopic value contribution of ice

during the Oligocene by 0.25‰ (Table 1). This in turn
 217 would have resulted in an isotopic value of calcite of
 218 $\sim 3.0\text{‰}$ for the Oligocene, which is consistent with 2°C
 219 bottom-water concomitant with a fully glaciated East
 220 Antarctic continent. Uncertainty in this value includes
 221 the possible effects of salinity. The range in salinity in
 222 the deep-sea today (e.g., North Atlantic Deep Water
 223

t1.1 Table 1

t1.2 Ice volume and resulting isotopic change to mean global ocean if the ice sheet melted

t1.3	Ice sheet	Volume (km^3)	Water volume km^3	Isotopic change (‰)		
				Present-day isotopic values	Isotopic value if all ice is -35‰	Isotopic value if all ice is -50‰
t1.4						
t1.5	Greenland	2,600,000	2,340,000	-0.07	-0.06	-0.09
t1.6	East Antarctic Ice sheet	26,039,200	23,435,280	-0.85	-0.60	-0.85
t1.7	West Antarctic ice sheet	3,262,000	2,935,800	-0.06	-0.07	-0.11
t1.8	Other Antarctic ice	808,600	727,740	-0.02	-0.02	-0.03
t1.9	Other ice	180,000	162,000	0.00	0.00	-0.01
t1.10	Total	32,889,800	29,600,820	-1.00	-0.75	-1.08
t1.11						
t1.12	$\delta^{18}\text{O}$ value of calcite with present-day ice volume and a bottom-water temperature of 2.0°C .					3.34
t1.13	Isotopic increase to oceans from Greenland and WIAS only					-0.13
t1.14	$\delta^{18}\text{O}$ value of deep-sea calcite with EAIS present and a bottom-water temperature of 2.0°C .					3.21
t1.15	Difference between present-day and Oligocene ice sheet isotopic contribution to ocean					-0.25
t1.16	$\delta^{18}\text{O}$ value of calcite an Oligocene EAIS and a bottom-water temperature of 2.0°C .					2.96

Note: that the following data are used here: the surface area of the ocean $\sim 362,000,000 \text{ km}^2$, the average ocean depth $\sim 3.8 \text{ km}$, and ocean volume $\sim 1,375,600,000 \text{ km}^3$.

t1.17

224 [34.95‰] and Antarctic Bottom Water [34.65‰] is
 225 about 0.3‰, resulting in uncertainty in $\delta^{18}\text{O}$ of approx-
 226 imately $\pm 0.1\text{‰}$. A warmer water mass with higher
 227 salinity would have a higher $\delta^{18}\text{O}$, resulting in an
 228 over-estimate in ice volume. In contrast, a colder
 229 deep-water mass with lower salinity, such as a proto-
 230 AABW, would have had a lower $\delta^{18}\text{O}$, resulting in an
 231 under-estimate of the ice volume. Recent studies have
 232 suggested that West Antarctica and perhaps even north-
 233 ern hemisphere continents may have been glaciated
 234 during the Oligocene (e.g., Coxall et al., 2005). How-
 235 ever, if a West Antarctic Ice Sheet (WAIS) existed
 236 during the Oligocene, its isotopic contribution would
 237 be minor (0.06‰), and the presence of northern hemi-
 238 sphere ice sheets during the Palaeogene has little evi-
 239 dence from the northern hemisphere fauna, flora, or
 240 lithological studies to support it (e.g., Wolfe, 1978;
 241 Wolfe and Poore, 1982; Axelrod and Raven, 1985;
 242 Tiffney, 1985). Even so, a fully developed Greenland
 243 ice sheet would increase the isotopic value of the global
 244 oceans by 0.07‰ and combined with a WAIS could be
 245 invoked to explain a small fraction of the larger ice
 246 volume estimates recently proposed for the Oligocene
 247 (equivalent to 80 m ASL, Kominz and Pekar, 2001; 90
 248 m ASL Lear et al., 2004; 100 to 160 m ASL, Coxall et
 249 al., 2005).

250 Apparent sea-level estimates were calculated using
 251 the $\delta^{18}\text{O}$ to ASL calibrations for Sites 689, 690, 744,
 252 929, and 1218 (Pekar et al., 2002; this study; Fig. 2).
 253 Isotopic values of $\geq 3\text{‰}$, which occur at each late
 254 Oligocene isotopic event, are used to indicate an ice
 255 sheet equivalent in size to the present-day EAIS. The
 256 calibrations are further refined at each isotopic event by
 257 comparing isotopic offsets among the $\delta^{18}\text{O}$ records,
 258 which is ascribed to temperature variability between
 259 ocean basins. For example, at Mi1, Sites 929 and
 260 1218 are $\sim 0.4\text{‰}$ lighter than Sites 1090, which is
 261 assumed to be due to cooler bottom-water bathing
 262 Site 1090.

263 Although previous calibrations indicate that temper-
 264 ature scales linearly with respect to ice volume, uncer-
 265 tainties in temperature variability still may exist. For
 266 example, bottom-water temperature changes could
 267 occur outside the variability suggested by the calibra-
 268 tions for a given site owing to long or short-term
 269 changes in deep-sea circulation patterns. Additionally,
 270 apparent sea-level/ice volume estimates from high $\delta^{18}\text{O}$
 271 values ($\geq 3\text{‰}$) are considered more robust, because
 272 these values are consistent with a fully glaciated East
 273 Antarctic continent and cold bottom-water tempera-
 274 tures, while lower $\delta^{18}\text{O}$ values could have a wider
 275 range of possible ice volume and bottom-water tem-

peratures. For example, the highest values at Site 1090
 are consistent with an ice sheet up to 25% larger than
 the present-day EAIS and bottom-water temperatures
 near or slightly colder than water temperatures currently
 bathing Site 1090 (Billups et al., 2002). In fact, to
 invoke a smaller ice volume would require the unlikely
 scenario of colder bottom-water occurring during the
 late Oligocene, a time with a warmer climate and a
 polythermal ice sheet, in contrast to the extreme cold
 polar conditions that exist in Antarctica today.

3. Deep-sea $\delta^{18}\text{O}$ records from the late Oligocene

Deep-sea $\delta^{18}\text{O}$ records in most oceanic basins show
 a significant ($> 1.0\text{‰}$) decrease after the $\delta^{18}\text{O}$ event
 (Oi2b) at 26.8 Ma, reaching their lowest values of the
 Oligocene by ~ 24.5 Ma (Fig. 3). For example, low-
 resolution $\delta^{18}\text{O}$ records from Atlantic Sites 522, 529,
 558, 563 (Miller et al., 1987, 1991) all indicate a
 decrease between 26.6 and 23.5 Ma, culminating with
 low $\delta^{18}\text{O}$ values between $\sim 2.0\text{‰}$ and 1.2‰ (Fig. 3).
 Low values in the high-resolution tropical Atlantic
 Ocean ODP Site 929 record extend from 25.2 Ma to
 immediately before the Mi1 event. A similar trend
 occurs in $\delta^{18}\text{O}$ record from tropical Pacific Ocean
 ODP Site 1218, with high $\delta^{18}\text{O}$ values (i.e., glacial
 maxima) decreasing by $\sim 1\text{‰}$ (Lear et al., 2004).
 These values are heavier than Site 929 on average by
 0.5‰ to 0.8‰, during $\delta^{18}\text{O}$ maxima and minima,
 respectively. Other Pacific Ocean ODP Sites 77 and
 803 show a decrease in $\delta^{18}\text{O}$ values of $\sim 1\text{‰}$ during the
 late Oligocene. These low $\delta^{18}\text{O}$ values have been used
 to suggest a warming event occurred during the late
 Oligocene coupled with a collapse of the Antarctic ice
 sheet (e.g., Zachos et al., 2001). These isotopic values
 are similar to middle Eocene values, a time usually
 considered to be mainly ice free (Zachos et al., 2001).
 Slightly higher values $\delta^{18}\text{O}$ (1.8‰ to 2.6‰) are
 recorded in South Atlantic Site 1090 (Billups et al.,
 2002) between 23.8 and 23.0 Ma, with the highest
 values just above the threshold requiring the presence
 of ice sheets (2.45‰; Miller et al., 1991).

Unlike the low $\delta^{18}\text{O}$ values observed in records in
 the Atlantic and Pacific Ocean basins, $\delta^{18}\text{O}$ values from
 Southern Ocean ODP Sites 689, 690, and 744 remain
 high ($\sim 3\text{‰}$). In the case of Site 690, they increase to
 3.1‰–3.3‰ in the upper portion of the record (25.2–
 24.5 Ma), with $\delta^{18}\text{O}$ records from Sites 744 and 689
 also containing relatively high values (2.9‰–3.0‰) at
 the top of their records (24.9 and 25.4 Ma, respective-
 ly). In contrast, between ~ 26.0 and 24.5 Ma, an isotopic
 gradient of $\sim 0.6\text{‰}$ to 1.6‰ developed between Site 690

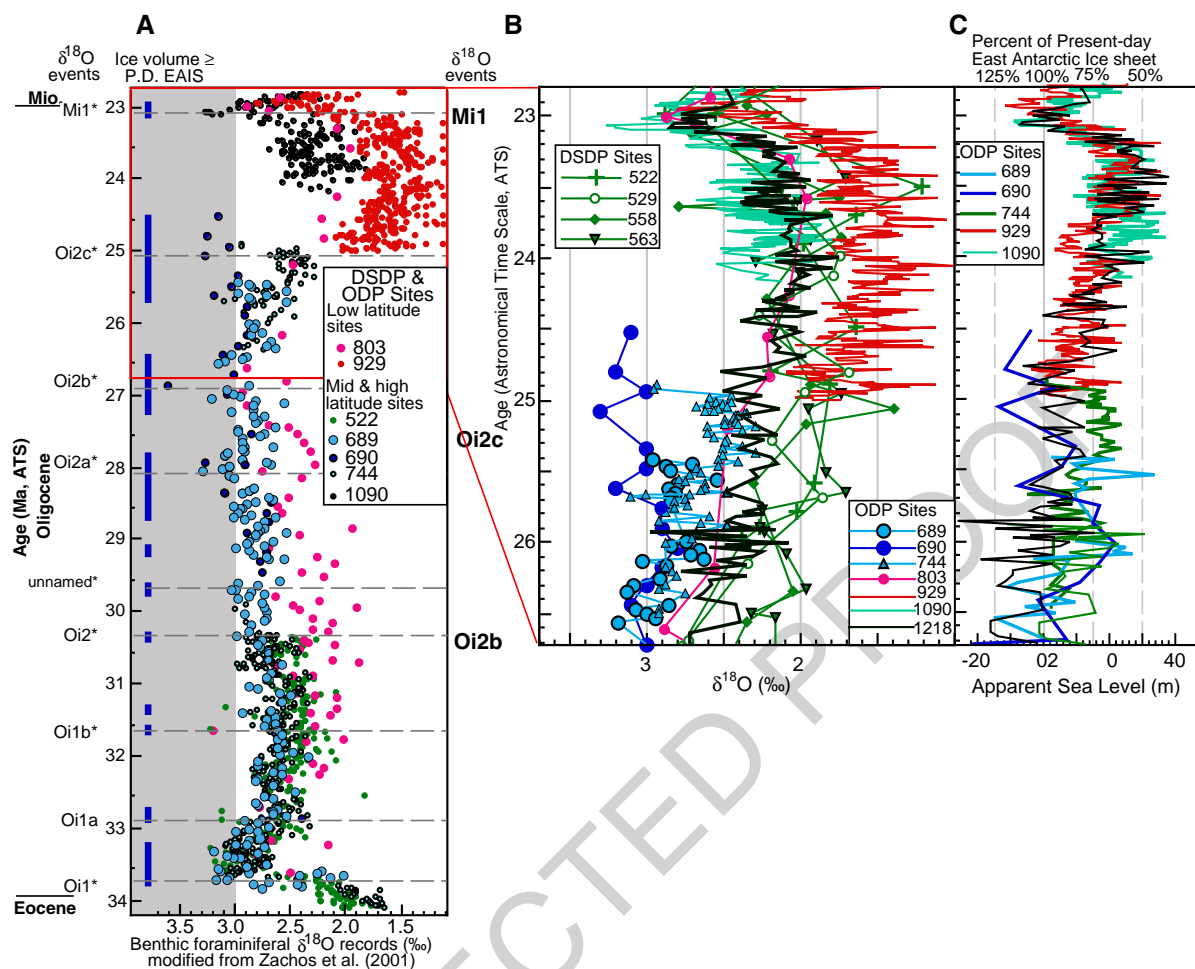


Fig. 3. (A) Oligocene benthic foraminiferal $\delta^{18}\text{O}$ records are from Barrera et al. (1993) and modified from Zachos et al. (2001). Blue circles are from Southern Ocean sites, green circles are from mid-latitude sites, and pink and red circles are from low latitude sites. The abrupt $\delta^{18}\text{O}$ decrease at circa 25.5 Ma is due to a change in the source of data from high latitude to low latitude sites, with Southern Ocean sites below and mainly western equatorial Atlantic Site 929 above (Pekar et al., 2002). (B) Oxygen isotope records for the late Oligocene showing the divergence in the records (from Barrera et al., 1993; modified from Zachos et al., 2001; Billups et al., 2002; Lear et al., 2004). Isotopic values of $\geq 3\text{‰}$ are consistent with carbonate that formed in water of $2.0\text{ }^{\circ}\text{C}$ concomitant with a fully glaciated Antarctic continent during the late Oligocene. Oxygen isotope values from *Cibicidoides* spp. are depleted relative to isotope equilibrium and were adjusted accordingly by 0.64‰ (Graham et al., 1981). On the left are $\delta^{18}\text{O}$ events from Miller et al. (1991) and Pekar and Miller (1996). (C) Apparent sea-level (ASL) estimates are derived from application of $\delta^{18}\text{O}$ to ASL calibrations to $\delta^{18}\text{O}$ records from Sites 689, 690, 744, 929, 1090, and 1218. The upper x-axis is the percent of the present-day EAIS (equivalent to ~ 60 m ASL). The lower x-axis is apparent sea-level change, with zero representing sea level resulting from ice volume equivalent to the present-day EAIS, with increasing values representing sea-level rise and negative numbers representing ice volume greater than the present-day EAIS volume.

326 (2.9‰ – 3.3‰) and North Atlantic Sites 529, 558, and
 327 563 (2.3‰ and 1.7‰), with the highest gradient (1.0‰
 328 to 2.0‰) occurring between Site 690 and Site 929
 329 between 25.0 and 24.5 Ma. Therefore, most of the
 330 abrupt late Oligocene $\delta^{18}\text{O}$ shift at ~ 25 Ma in the
 331 composite record of Zachos et al. (2001) is due to a
 332 change in the location of the data source, with values
 333 younger than 25 Ma being mainly from Atlantic Ocean
 334 Site 929 and values older than 25 Ma being from mid-
 335 latitude and Southern Ocean sites (Pekar et al., 2002;

Lear et al., 2004). Additionally, a significant gradient 336
 also develops between Sites 690 and the only high- 337
 resolution record that extends throughout the late Oligo- 338
 cene, tropical Pacific Ocean Site 1218, ranging from 339
 $\sim 0.5\text{‰}$ to 1.2‰ near the top of the record at Site 690. 340
 Furthermore, no significant changes in isotopic values 341
 occur in the Site 1218 record above the top of the Site 342
 690 record (24.5 Ma), supporting the idea that a large 343
 gradient ($> 1\text{‰}$) developed between the Weddell Sea 344
 (i.e., Site 690) and sites located in the Atlantic Basin. In 345

summary, while aliasing is always a factor when comparing low-resolution records, it is clear that a significant $\delta^{18}\text{O}$ gradient developed during the late Oligocene between the Weddell Sea Sites and from the Atlantic (from 1.0‰ up to 2.0‰, equivalent to 4–8 °C) and to a lesser extent from the Pacific Ocean (~0.6‰ to ~1.0‰, equivalent to ~2–4 °C). This gradient is at least partly responsible for the significant decrease seen in other composite records (Miller et al., 1987; Abreu and Anderson, 1998), owing to that these composite records were biased to isotopic records from Atlantic Ocean Sites. These large $\delta^{18}\text{O}$ gradients allowed an evaluation of changing deep-sea water masses through the late Oligocene. In contrast, identifying deep-water masses using $\delta^{13}\text{C}$ records during the late Oligocene and early Miocene is difficult because basin-to-basin gradients were small (e.g., Woodruff and Savin, 1989; Wright et al., 1992; Wright and Miller, 1993). These small gradients have been ascribed to low mean ocean nutrient levels (Billups et al., 2002).

4. Deep-sea water mass distribution changes during the late Oligocene

Construction of three $\delta^{18}\text{O}$ transects for Oi-events Oi2b (27.0–26.6 Ma), Oi2c (25.2–24.8 Ma), and Mil (23.2–22.8 Ma) indicates that a significant water mass redistribution occurred during the late Oligocene (Fig. 4). A 400 ky time slice is used here to ensure that the maximum isotopic value of the $\delta^{18}\text{O}$ event is captured. The maximum $\delta^{18}\text{O}$ value from each site is used for the time slices as it should be the most representative of the $\delta^{18}\text{O}$ event. Although, low-resolution records often may not capture the highest value at an isotopic event, these isotopic transects do provide an indication of the broad changes that occurred at each event. Each of the time slices contains isotopic values of $\geq 3.0\text{‰}$, which are consistent with carbonate forming in cold bottom-water (≤ 2.0 °C) concomitant with a fully glaciated EAC. At 26.8 Ma, the highest $\delta^{18}\text{O}$ values are found at the Weddell Sea Sites ($> 3\text{‰}$), with slightly lower values in the Pacific and Indian basins (2.6‰–2.9‰) and Atlantic basin (2.3‰–3.0‰). Using $\delta^{18}\text{O}$ to ASL calibrations, a bottom-water temperature of 1.0–2.0 °C is estimated for the Weddell Sea (based on $\delta^{18}\text{O}$ values 3.0‰–3.6‰), with 2–4 °C in the Pacific and Indian Oceans and 2–5 °C at the Atlantic Sites. In contrast, during the Oi2c event, $\delta^{18}\text{O}$ values in the Southern Ocean (i.e., Sites 689, 690, and 744) remain high (2.9‰–3.3‰), while values in the Atlantic basin decreased by 0.5‰ to 1.0‰ (Fig. 4). This results in an isotopic gradient between the Southern and Atlantic

Oceans of 1.0‰ to 1.2‰ (equivalent to ~4 to 5 °C, if the entire increase was due to temperature). This suggests that a second deep-water mass developed during the late Oligocene and replaced the colder deep-water in much of the ocean basins as suggested by the heavy isotopic values observed at Oi-event Oi2b. However, warmer water without increased salinity would have insufficient density to become a deep-water mass and compete with a colder dense water mass originating from Antarctica. If a bottom-water mass near Antarctic during the Oligocene were ~2 °C, with similar salinities as the present-day Antarctic Bottom Water (34.65‰; Wright and Colling, 1995), a bottom-water with a temperature of ~7 °C would require a salinity ~0.6‰ higher to have a similar density as the deep-water near Antarctica (based on Wright and Colling, 1995). This would result in an isotopic increase of ~0.2‰ (using 1.0‰ salinity=0.3‰ $\delta^{18}\text{O}$), which would offset the temperature increase by 0.8 °C. Therefore, a large portion of deep-water temperatures in the Atlantic basin could have been ~7 °C or greater, based on a bottom-water temperature of 2.0 °C (based on values of 2.9‰ and 3.2‰) in the deep-water at Sites 690 and 744. These bottom-water temperatures are warmer than at any other time during the Oligocene and are similar to temperatures estimated during the middle Eocene (e.g., Miller et al., 1987; Zachos et al., 2001). It should also be noted that $\delta^{18}\text{O}$ values from Site 744 decrease slightly (2.7‰–2.3‰) and diverge by ~0.5‰ (equivalent to ~2 °C) from records from the Weddell Sea between 25.6 and 25.1 Ma before returning to similarly high values (~3‰) at 25.0 Ma. This suggests that slightly warmer deep-water may also have briefly bathed this region of the Southern Ocean during this time. During the Mil event, increasing $\delta^{18}\text{O}$ values indicate colder water once again filled most of the Atlantic basin, with the highest values (3.0‰–3.3‰) (and presumably coldest water) being found in the deepest part of the basin at Southern Atlantic Site 1090 and Southern Indian Ocean Site 704 (Fig. 4). Hiatuses at Sites 689, 690, and 744 prevented us from evaluating the spatial extent of colder Southern Component Water during this time interval. In contrast to the Oi2c event, warmer water at the Oligocene/Miocene boundary became restricted to intermediate water depths in the Indian and Atlantic Oceans.

5. Estimates of ice volume changes during the late Oligocene

Late Oligocene (26–23 Ma) ice volume estimates are equivalent to ~50% to 125% of present-day EAIS,

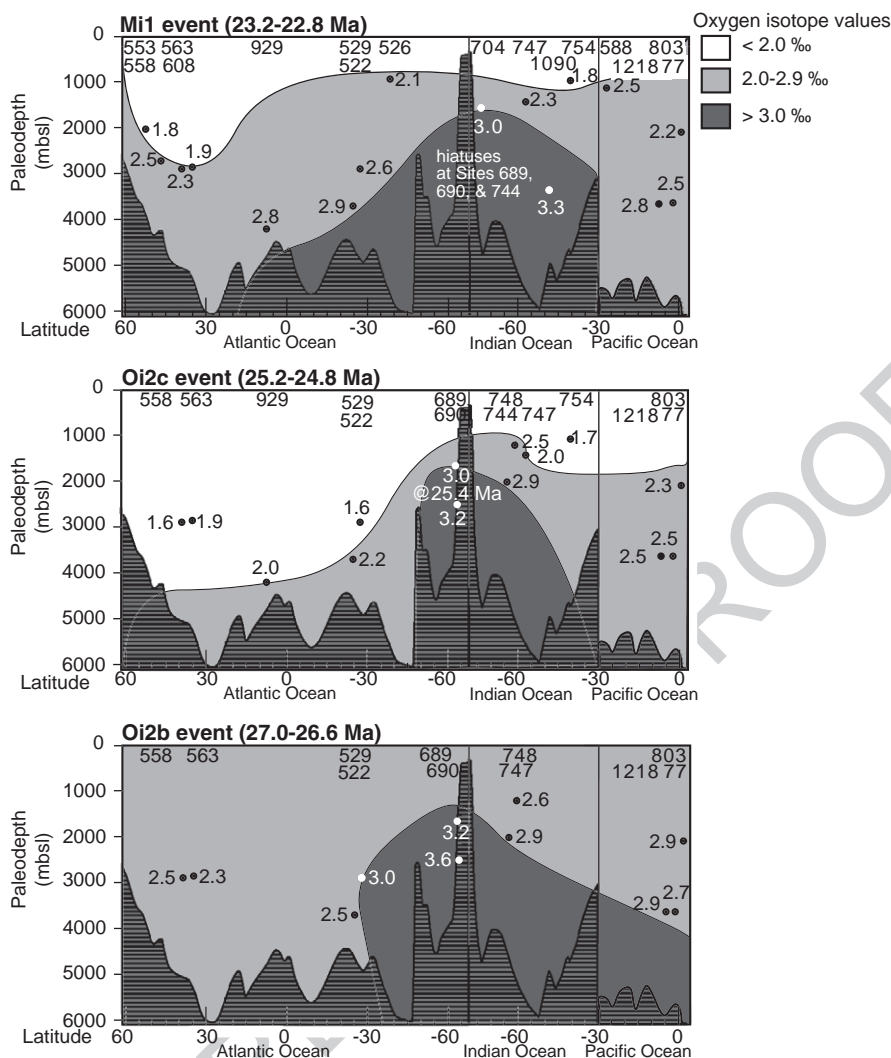


Fig. 4. Oxygen isotope transects for the Atlantic Ocean, Indian Ocean, and Pacific Oceans are constructed at three oxygen isotope events: (A) Oi2b (26.8 Ma), (B) Oi2c (25.1 Ma), and (C) Mi1 (23.0 Ma). DSDP and ODP sites used for each transect are labeled in the upper portion of each transect. Paleodepths for each site are indicated next to circles. Oxygen isotopic values shown next to the circles represent the maximum values within the 400-ky time slice. In each of the isotopic transects, cold deep-water ($\geq 3.0\text{‰}$) is generally restricted to the Southern Ocean. In contrast, warmer water ($< 2.0\text{‰}$) becomes an important water mass in the Atlantic and Indian Oceans during Oi-event Oi2c (circa 25.1 Ma). Note that the top of the record from Site 689 ends ~ 200 ky below the time slice for Oi2c event.

446 during glacial minima and maxima, respectively. High
 447 $\delta^{18}\text{O}$ values (2.9‰–3.3‰) consistent with a heavily
 448 glaciated EAC occurred at the top of the records at all
 449 three Southern Ocean sites (ODP Sites 689, 690, and
 450 744) between 25.4 and 24.5 Ma (Fig. 3B). Between
 451 25.0 and 24.5 Ma, an offset of $\sim 1.2\text{‰}$ exists between
 452 average $\delta^{18}\text{O}$ values from Site 690 and maximum
 453 values from Site 929. The new chronology by Flor-
 454 indo and Roberts (2004) provides a much higher
 455 confidence that the average values at Site 690 between
 456 25.0 and 24.5 Ma correlate to the maximum values at
 457 Site 929, therefore permitting ice volume during the

latest Oligocene to be constrained using the calibrated 458
 record from Site 929. A 1.0‰ decrease occurs 459
 between the high (glacial periods) and lowest $\delta^{18}\text{O}$ 460
 values (interglacial periods) from Site 929 from 25.0 461
 to 24.0 Ma, which is equivalent to an ice volume 462
 decrease of 50% of the present-day EAIS. During 463
 the Mi1 event, the record from Site 1090 contains 464
 values (3.3‰; Billups et al., 2002) consistent with a 465
 return to a fully glaciated EAC, being perhaps 15% 466
 larger than the present-day EAIS. Therefore, increas- 467
 ing $\delta^{18}\text{O}$ values at Sites 929 and 1218 between 23.5 468
 and 23.0 Ma are attributed to mainly bottom-water 469

470 cooling concomitant with an increase in ice volume
471 equivalent to ~40 m ASL fall.

472 The resolution of the $\delta^{18}\text{O}$ record from Site 929
473 (Zachos et al., 2001) is sufficiently high to resolve
474 cycles that have been attributed to the 41 ky obliquity
475 cycle. This permitted evaluation of Antarctic ice vol-
476 ume variability at the 10^4 yr timescale. Variability in the
477 $\delta^{18}\text{O}$ record attributed to obliquity-forcing suggests
478 changes in ice volume from 80% of the modern EAIS
479 during glacial periods to 50% during interglacial peri-
480 ods. This range in variability is equivalent to ~20 m
481 change in ASL and is generally consistent with orbitally
482 forced ice sheet simulations under higher than present
483 atmospheric CO_2 (DeConto and Pollard, 2003b).

484 6. Resolving the conundrum of warm deep-water 485 concomitant with a glaciated Antarctica

486 The conundrum of low $\delta^{18}\text{O}$ values and a large ice
487 sheet on Antarctica can be resolved by inferring the
488 existence of at least two deep-water masses during the
489 late Oligocene, one originating from near Antarctica
490 and typically described as proto-Antarctic Bottom
491 Water (proto-AABW) and a second warmer (and pre-
492 sumably more saline) water mass that strengthened after
493 27 Ma. It appears from $\delta^{18}\text{O}$ records from the Weddell
494 Sea and other ocean basins that most of the time the
495 colder proto-AABW was not the dominant deep-water
496 mass outside the Weddell Sea. This suggests that this
497 deep-water became entrained into and mixed with the
498 warmer deep-water mass as it moved away from the
499 Weddell Sea. The only exceptions occurred during Oi-
500 events, Oi2b and Mi1, when colder deep-water filled
501 the deep ocean basins (Fig. 4). During these glacial
502 events, the expansion of the Antarctic ice sheet near the
503 coastlines would have contributed to colder surface
504 water temperatures and expanded sea ice cover, which
505 likely impacted deep-water formation around Antarc-
506 tica. This could have resulted in the strengthening of a
507 proto-AABW during periods when the ice was at its
508 maximum. In contrast, during glacial minima, retreat of
509 the ice sheet into the continental interior would have
510 resulted in a reduction of sea ice and warmer water
511 temperatures along the coastline, leading to a reduction
512 in proto-AABW production. Furthermore, additional
513 runoff from a retreating ice sheet during interglacials
514 would result in a freshening of the coastal water around
515 Antarctic, further weakening proto-AABW production.
516 This suggests that the large temperature gradient among
517 deep-sea sites during the late Oligocene was the result
518 of decreased production of proto-AABW and perhaps
519 an increase in the production of warmer deep-water,

and not a cooling of proto-AABW as a result of the
opening of the Drake Passage and subsequent isolation
of the Southern Ocean as previously suggested (Billups
et al., 2002).

A number of numerical modeling simulation studies
that tested the effects of open versus closed Southern
Ocean gateways on ocean circulation and climate have
yielded results that support the idea that as the Drake
Passage opened, Southern Ocean deep-water formation
(i.e., proto-AABW) decreased, high southern latitude
temperatures decreased, and a warmer deep-water mass
developed in the northern hemisphere (i.e., proto-North
Atlantic Deep Water, proto-NADW) (Mikolajewicz et
al., 1993; Toggweiler and Samuels, 1995; Nong et al.,
2000; Toggweiler and Bjornsson, 2000; Huber et al.,
2004; Sijp and England, 2004). The Drake Passage was
likely the final barrier to circum-Antarctic circulation,
opening in the early Oligocene (Lawver and Gahagan,
1998), and began providing a deep-water passage
somewhat later in the Oligocene (Livermore et al.,
2004). Sijp and England (2004), using an ocean general
circulation model coupled to a simple climate model,
showed that while high Southern Latitude SSTs cooled
by several degrees when the Drake Passage opened,
Southern Hemisphere deep-water formation (i.e., proto-
AABW) slowed by ~75%, with little or no NADW until
the passage opened, with significant NADW production
beginning only after a deep circum-Antarctic passage
was established. The simulations indicate that the turn-
ing on of NADW warmed the intermediate and deep
ocean north of 30° South by ~2 °C. In the model, North
Atlantic sea surface salinity also increased by ~1 psu,
mostly in response to ocean circulation, rather than
fresh water forcing at the surface. These results support
the conclusions in this paper of reduced proto-AABW
formation, strengthening of a warmer deep-water mass,
and a cold and heavily glaciated East Antarctic conti-
nent occurring during the late Oligocene.

The Tethys has been suggested as a possible source
of warmer water during the early Miocene (e.g., Brass
et al., 1982; Woodruff and Savin, 1989). Isotopic evi-
dence suggests that during the early Miocene, warmer
deep to intermediate water formed in the Tethys and
then entered the Indian Ocean (Woodruff and Savin,
1989; Wright and Miller, 1993). Warmer deep-water
inferred by the low $\delta^{18}\text{O}$ values from Atlantic Ocean
sites during the late Oligocene may represent the initi-
ation of a warmer (and presumably more saline) deep-
water mass, which may be analogous to the warmer
water postulated to have originated from the Tethys in
the early Miocene by Woodruff and Savin (1989).
However, during the Oligocene, warm water appears

572 to have originated in the Atlantic and not the Indian
573 Ocean, as in the early Miocene.

574 Furthermore, high $\delta^{18}\text{O}$ values from Weddell Sea
575 sites (3.0‰–3.3‰) occurred at times when most ocean
576 basins contained $\delta^{18}\text{O}$ values that were similar to the
577 low early Miocene $\delta^{18}\text{O}$ values. This suggests that the
578 late Oligocene model of a spatially restricted proto-
579 AABW, an expanded warmer deep-water mass, and a
580 heavily glaciated East Antarctica may have also been
581 true for the early Miocene (Pekar and DeConto, this
582 issue). This may explain the evidence for cold, tundra-
583 like conditions on the Ross Sea margin and continental
584 glaciation, as inferred from proximal Antarctic records
585 during this time interval (Raine, 1998; CRST, 1998;
586 Roberts et al., 2003) as well as ice grounding lines
587 across the Antarctic shelf in areas such as the Ross
588 Sea and Prydz Bay (Cooper et al., 1991; Bartek et al.,
589 1997). This contrasts with previous interpretations of
590 Antarctic warming during the early Miocene based on
591 $\delta^{18}\text{O}$ records and is also consistent with recent numer-
592 ical modeling studies (DeConto and Pollard, 2003a,b),
593 which showed how significant Antarctic ice can exist
594 during times with warmer-than-present-day global
595 mean temperatures, and poleward ocean heat transport.

596 Acknowledgments

597 This research was supported by National Science
598 Foundation grants (OCE 99-11121 to N. Christie-
599 Blick and S.F. Pekar). We thank P. Barrett, A. Viladrich,
600 P. Wilson, J. Wright, and two anonymous reviewers for
601 providing comments on an earlier version of this man-
602 uscript. We thank C. Lear and K. Billups for sharing
603 their isotopic data. This is Lamont-Doherty Earth Ob-
604 servatory Contribution Number 0000.

605 References

606

607 Abreu, V.S., Anderson, J.B., 1998. Glacial eustasy during the Ceno-
608 zoic: sequence stratigraphic implications. *American Association*
609 *of Petroleum Geologists Bulletin* 82, 1385–1400.
610 Axelrod, D.I., Raven, P.H., 1985. Origins of the Cordilleran flora.
611 *Journal of Biogeography* 12, 21–47.
612 Barrera, E., Baldauf, J., Lohmann, K.C., 1993. Strontium isotope and
613 benthic foraminifer stable isotopic results from Oligocene sedi-
614 ments at Site 803. In: Berger, W.H., Kroenke, L.W., Mayer, L.A.
615 (Eds.), *Proceedings of the Ocean Drilling Program, Scientific*
616 *Results, Leg. vol. 130. Ocean Drilling Program, College Station,*
617 *Texas*, pp. 269–279.
618 Barrett, P.J. (Ed.), 1989. Antarctic Cenozoic history from CIROS-1
619 drillhole, McMurdo Sound, DSIR Bulletin, vol. 245. Scientific
620 Information Publishing Centre, Wellington (254 pp.)
621 Bartek, L.R., Andersen, J.L.R., Oneacre, T.A., 1997. Substrate control
622 on distribution of subglacial and glaciomarine seismic facies

based on stochastic models of glacial seismic facies deposition 623
on the Ross Sea continental margin, Antarctica. *Marine Geology* 624
143, 223–262. 625
Billups, K., Channell, J.E.T., Zachos, J., 2002. Late Oligocene to 626
early Miocene geochronology and paleoceanography from the 627
subantarctic South Atlantic. *Paleoceanography* 17, doi:10.1029/ 628
2000PA000568. 629
Brass, G.W., Southam, J.R., Peterson, W.H., 1982. Warm saline 630
bottom water in the ancient ocean. *Nature* 296, 620–623. 631
Cape Roberts Science Team, 1998. Initial Report on CRP-1, Cape 632
Roberts Project, Antarctica. *Terra Antarctica* 5 (187 pp.). 633
Cape Roberts Science Team, 1999. Studies from the Cape Roberts 634
Project, Ross Sea, Antarctica, Initial Report on CRP-2/2A. *Terra* 635
Antartica 6 (187 pp.). 636
Cape Roberts Science Team, 2000. Studies from the Cape Roberts 637
Project, Ross Sea, Antarctica, Initial Report on CRP-3. *Terra* 638
Antartica 7 (209 pp.). 639
Cooper, A.K., Barrett, P.J., Hinz, K., Traube, V., Leitchenkov, G., 640
Stagg, H.M.J., 1991. Cenozoic prograding sequences of the Ant- 641
arctic continental margin: a record of glacio-eustatic and tectonic 642
events. *Marine Geology* 102, 175–213. 643
Coxall, H.K., Wilson, P.A., Palike, H., Lear, C.H., Backman, J., 2005. 644
Rapid stepwise onset of Antarctic glaciation and deeper calcite 645
compensation in the Pacific Ocean. *Nature* 433, 53–57. 646
DeConto, R.M., Pollard, D., 2003a. Rapid Cenozoic glaciation of 647
Antarctica induced by declining atmospheric CO₂. *Nature* 421, 648
245–249. 649
DeConto, R.M., Pollard, D., 2003b. A coupled climate-ice sheet 650
modeling approach to the early Cenozoic history of the Antarctic 651
ice sheet. *Palaeogeography, Palaeoclimatology, Palaeoecology* 652
198, 39–52. 653
Denton, G.H., Hughes, T.J., 2002. Reconstructing the Antarctic ice 654
sheet at the last glacial maximum. *Quaternary Science Reviews* 655
21, 193–202. 656
Florindo, F., Roberts, A.P., 2005. Eocene–Oligocene magnetobiochro- 657
nology of ODP Sites 689 and 690, Maud Rise, Weddell Sea, 658
Antarctica. *Geological Society of America Bulletin* 117, 46–66. 659
Graham, D.W., Corliss, B.H., Bender, M.L., Keigwin, L.D., 1981. 660
Carbon and oxygen isotopic disequilibrium of recent benthic for- 661
aminifera. *Marine Micropaleontology* 6, 483–497. 662
Hay, W.W., DeConto, R., Wold, C.N., Wilson, K.M., Voigt, S., 663
Schulz, M., Wold-Rosby, A., Dullo, W.-C., Ronov, A.B., Balu- 664
khovsky, A.N., Soeding, E., 1999. Alternative global Cretaceous 665
paleogeography. In: Barrera, E., Johnson, C. (Eds.), *The Evolution* 666
of Cretaceous Ocean/Climate Systems. Geological Society of 667
America Special Paper, vol. 332, pp. 1–47 ([http://www.odsns.de/](http://www.odsns.de/odsns/services/paleomap/paleomap.html) 668
[odsns/services/paleomap/paleomap.html](http://www.odsns.de/odsns/services/paleomap/paleomap.html)). 669
Huber, M., Brinkhuis, H., Stickley, C.E., Doos, L., Sluijs, A., War- 670
naar, J., Schellenberg, S.A., Williams, G.L., 2004. Eocene circula- 671
tion of the Southern Ocean: was Antarctica kept warm by 672
subtropical waters? *Paleoceanography* 19, A4026. 673
Huybrechts, P., 2002. Sea-level changes at the LGM from ice- 674
dynamic reconstructions of the Greenland and Antarctic ice 675
sheets during the glacial cycles. *Quaternary Science Reviews* 676
21, 203–231. 677
Kennett, J.P., Stott, L.D., 1990. Proteus and proto-Oceanus: Paleo- 678
gene oceans as revealed from Antarctic stable isotopic results. 679
ODP Leg 113. *Proceedings of the Ocean Drilling Program Sci-* 680
entific Results 94, 1217–1244. 681
Kominz, M.A., Pekar, S.F., 2001. Oligocene eustasy from two-di- 682
mensional sequence stratigraphic backstripping. *Geological Soci-* 683
ety of America Bulletin 113, 291–304. 684

- 685 Laskar, J., Robutel, P., Joutel, F., Gastineau, M., Correia, A.,
686 Levrard, B., 2005. A long term numerical solution for the
687 insolation quantities of the Earth. *Astronomy and Astrophysics*
688 428, 261–286, doi:10.1051/0004-6361:20041335.
- 689 Lawver, L.A., Gahagan, L.M., 1998. Opening of Drake passage and
690 its impact on Cenozoic ocean circulation. In: Crowley, T.J., Burke,
691 K.C. (Eds.), *Tectonic Boundary Conditions for Climate Recon-*
692 *structions*. Oxford University Press, New York, pp. 212–223.
- 693 Lear, C.H., Elderfield, H., Wilson, P.A., 2000. Cenozoic deep-sea
694 temperature and global ice volumes from Mg/Ca in benthic for-
695 aminiferous calcite. *Science* 287, 269–272.
- 696 Lear, C.H., Rosenthal, Y., Coxall, H.K., Wilson, P.A., 2004. Late
697 Eocene to early Miocene ice sheet dynamics and the global carbon
698 cycle. *Paleoceanography* 19, A4015, doi:10.1029/2004PA001039.
- 699 Livermore, R., Eagles, G., Morris, P., Maldonado, A., 2004. Shack-
700 leton fracture zone: no barrier to early circumpolar ocean cir-
701 culation. *Geology* 32, 797–800.
- 702 Mikolajewicz, U., Maier-Reimer, E., Crowley, T.J., Kim, K.-Y., 1993.
703 Effect of Drake and Panamanian gateways on the circulation of an
704 ocean model. *Paleoceanography* 8 (4), 409–426.
- 705 Miller, K.G., Fairbanks, R.G., 1983. Evidence for Oligocene-Middle
706 Miocene abyssal circulation changes in the western North Atlan-
707 tic. *Nature* 306, 250–253.
- 708 Miller, K.G., Thomas, E., 1985. Late Eocene to Oligocene benthic
709 isotopic record, Site 574, Equatorial Pacific. *Initial Report Deep*
710 *Sea Drilling Project* 85, 981–996.
- 711 Miller, K.G., Fairbanks, R.G., Mountain, G.S., 1987. Tertiary oxygen
712 isotope synthesis, sea-level history, and continental margin ero-
713 sion. *Paleoceanography* 2, 1–19.
- 714 Miller, K.G., Feigenson, M.D., Kent, D.V., Olsson, R.K., 1988.
715 Oligocene stable isotope ($^{87}\text{Sr}/^{86}\text{Sr}$, $\delta^{18}\text{O}$, $\delta^{13}\text{C}$) standard section.
716 *Deep Sea Drilling Project. Paleoceanography* 3, 223–233.
- 717 Miller, K.G., Wright, J.D., Fairbanks, R.G., 1991. Unlocking the
718 icehouse: Oligocene–Miocene oxygen isotopes, eustasy, and mar-
719 gin erosion. *Journal of Geophysical Research* 96, 6,829–6,848.
- 720 Naish, T.R., Wolfe, K.J., Barrett, P.J., Wilson, G.S., Cliff, A.,
721 Bohaty, S.M., Buckler, C.J., Claps, M., Davey, F.J., Dunbar,
722 G.B., Dunn, A.G., Fielding, C.R., Florindo, F., Hannah, M.J.,
723 Harwood, D.M., Henrys, S.A., Krissek, L.A., Lavelle, M., van
724 der Meer, J., McIntosh, W.C., Niessen, F., Passchier, S., Powell,
725 R.D., Roberts, A.P., Sagnotti, L., Scherer, R.P., Strong, P.C.,
726 Talarico, F., Verosub, K.L., Villa, G., Watkins, D.K., Webb, P-
727 N., Wonik, T., 2001. Orbitally induced oscillations in the East
728 Antarctic ice sheet at the Oligocene/Miocene boundary. *Nature*
729 413, 719–723.
- 730 Nong, G.T., Najjar, R.G., Seidov, D., Peterson, W., 2000. Simulation
731 of ocean temperature change due to the opening of Drake Passage.
732 *Geophysical Research Letters* 27, 2689–2692.
- 733 Pekar, S.F., DeConto, R., this issue. High-Resolution Ice-Volume
734 Estimates for the Early Miocene: Evidence for a Dynamic
735 Ice Sheet in Antarctica, *Palaeogeography, Palaeoclimatology,*
736 *Palaeoecology*.
- 737 Pekar, S.F., Kominz, M.A., 2001. Two-dimensional paleoslope mod-
738 eling: a new method for estimating water depths for benthic
739 foraminiferal biofacies and paleo shelf margins. *Journal of Sedi-*
740 *mentary Research* 71, 608–620.
- 741 Pekar, S., Miller, K.G., 1996. New Jersey Oligocene “Icehouse”
742 sequences (ODP Leg 150X) correlated with global $\delta^{18}\text{O}$ and
743 Exxon eustatic records. *Geology* 24, 567–570.
- 744 Pekar, S.F., Christie-Blick, N., Kominz, M.A., Miller, K.G., 2002.
745 Calibrating eustasy to oxygen isotopes for the early icehouse
746 world of the Oligocene. *Geology* 30, 903–906.
- Prebble, J.G., Raine, J.I., Barrett, P.J., Hannah, M.J., this issue. 747
Vegetation and climate from two Oligocene glacioeustatic sedi- 748
mentary cycles (31 and 24 Ma) cored by the Cape Roberts Project, 749
Victoria Land Basin, Antarctica. *Palaeogeography, Palaeoclima-* 750
tology, Palaeoecology. 751
- Raine, J.I., 1998. Terrestrial palynomorphs from Cape Roberts Proj- 752
ect drillhole CRP-1, Ross Sea, Antarctica. *Terra Antarctica* 5, 753
539–548. 754
- Raine, J.I., Askin, R.A., 2001. Oligocene and Early Miocene terres- 755
trial palynology of the Cape Roberts Drillhole CRP-2/2A, Victoria 756
Land Basin, Antarctica. *Terra Antarctica* 7, 389–400. 757
- Ritz, C.V., Rommelaere, V., Dumas, C., 2001. Modeling the evolution 758
of Antarctic ice sheet over the last 420,000 years: implications for 759
altitude changes in the Vostok region. *Journal of Geophysical* 760
Research 106 (D23), 31943–31964. 761
- Roberts, A.P., Wilson, G.S., Harwood, D.M., Verosub, K.L., 2003. 762
Glaciation across the Oligocene–Miocene boundary in Southern 763
McMurdo Sound, Antarctica: new chronology from the CIROS-I 764
drill hole. *Palaeogeography, Paleoclimatology, Palaeoecology* 765
198, 113–130. 766
- Shackleton, N.J., Kennett, J.P., 1975. Late Cenozoic oxygen and 767
carbon isotopic changes at DSDP Site 284: implications for 768
glacial history of the Northern hemisphere and Antarctic. In: 769
Kennett, J.P., Houtz, R.E., et al., (Eds.), *Initial Reports of the* 770
Deep Sea Drilling Project, vol. 29, pp. 801–808. 771
- Sijp, W.P., England, M.H., 2004. Effect of the Drake Passage through 772
flow on Global Climate. *Journal of Physical Oceanography* 34, 773
1254–1266. 774
- Speiss, V., 1990. Cenozoic Magnetostratigraphy of Leg 113 drill sites, 775
Maude Rise, Weddell Sea, Antarctica. In: Barker, P.F., Kennett, 776
J.P. (Eds.), *Proceedings of the Ocean Drilling Program, Scientific* 777
Results, vol. 113, pp. 261–315. 778
- Tiffney, B.H., 1985. The Eocene North Atlantic land bridge: its 779
importance in Tertiary and modern phytogeography of the 780
Northern Hemisphere. *Journal of the Arnold Arboretum* 66, 781
243–273. 782
- Thomas, E., Zahn, R., Diester-Hauss, L., 1995. The Eocene–Oligo- 783
cene transition at high latitudes: benthic foraminifera, sediments 784
and stable isotopes. *EOS Transactions* 76 (Supplement), S187. 785
- Thorn, V.C., 2001. Oligocene and Early Miocene phytoliths from 786
CRP-2/2A and CRP-3, Victoria Land Basin, Antarctica. *Terra* 787
Antarctica 8, 407–422. 788
- Toggweiler, J.R., Bjornsson, H., 2000. Drake Passage and paleocli- 789
mate. *Journal of Quaternary Science* 15, 319–328. 790
- Toggweiler, J.R., Samuels, B., 1995. Effect of Drake Passage on the 791
global thermohaline circulation. *Deep-Sea Research* 42, 477–500. 792
- Williams, R.S., Ferrigno, J.G., 1999. *Satellite Image Atlas of Glaciers* 793
of the World, Chapter A: Introduction. U.S. Geological Survey 794
Professional Paper 1386-A. 795
- Wolfe, J.A., 1978. A paleobotanical interpretation of Tertiary climates 796
in the Northern Hemisphere. *American Scientist* 66, 694–704. 797
- Wolfe, J.A., Poore, R.Z., 1982. Tertiary marine and nonmarine cli- 798
matic trends. In: Crowell, J.C., Berger, W. (Eds.), *Pre-Pleistocene* 799
Climates, pp. 154–158 (Washington). 800
- Woodruff, F., Savin, S.M., 1989. Miocene deep-water oceanography. 801
Paleoceanography 4, 87–140. 802
- Wright, J., Colling, A., 1995. *Seawater: Its Composition, Properties,* 803
and Behaviour. Open University Press and Elsevier Science Ltd., 804
Oxford, 168. 805
- Wright, J.D., Miller, K.G., 1993. Southern ocean influences on late 806
Eocene to Miocene deep water circulation. *American Geophysical* 807
Union, Antarctic Research Series 60, 1–25. 808

- 809 Wright, J.D., Miller, K.G., Fairbanks, R.G., 1992. Early and middle
810 Miocene stable isotopes: implication for deep-water circulation
811 and climate. *Paleoceanography* 7, 357–387. 815
- 812 Zachos, J.C., Berggren, W.A., Aubry, M.P., Mackensen, A., 1992. 816
813 Isotope and trace element geochemistry of Eocene and Oligocene
814 Foraminifers from Site 748, Kerguelen Plateau. In: Schlich, R.,
820 Wise Jr., S.W., et al. (Eds.), Proc. ODP, Scientific Results, vol. 817
120. Ocean Drilling Program, College Station, TX, pp. 839–854. 818
Zachos, J.C., Pagani, M., Sloan, L., Thomas, E., Billups, K., 2001. 819
Trends, rhythms and aberrations in global climate 65 Ma to
present. *Science* 292, 686–693.

UNCORRECTED PROOF